ResearchGate

See discussions, stats, and author profiles for this publication at: https://www.researchgate.net/publication/265135418

# Hydrophobizing coatings for cultural heritage. A detailed study of resin/stone surface interaction

**Article** *in* Applied Physics A · July 2014

DOI: 10.1007/s00339-013-8127-z

CITATIONS
19

READS
213

**7 authors**, including:

Paola Fermo
University of Milan
**128** PUBLICATIONS **2,536** CITATIONS

SEE PROFILE

Saulius Kaciulis
Italian National Research Council
**283** PUBLICATIONS **3,040** CITATIONS

SEE PROFILE

Marco Brucale
Italian National Research Council
**64** PUBLICATIONS **869** CITATIONS

SEE PROFILE

**Some of the authors of this publication are also working on these related projects:**



electronic odor identification system View project



Landscape Archaeology in Northern Africa View project

All content following this page was uploaded by Saulius Kaciulis on 02 September 2014.

The user has requested enhancement of the downloaded file.

Appl. Phys. A (2014) 116:341–348
DOI 10.1007/s00339-013-8127-z

**Applied Physics A**
**Materials Science & Processing**

# Hydrophobizing coatings for cultural heritage. A detailed study of resin/stone surface interaction

**P. Fermo · G. Cappelletti · N. Cozzi · G. Padeletti · S. Kaciulis · M. Brucale · M. Merlini**

Received: 5 August 2013 / Accepted: 29 October 2013 / Published online: 22 November 2013
© Springer-Verlag Berlin Heidelberg 2013

**Abstract** Conservation of historical buildings is an important issue and the environmental conditions seriously affect the monument's stones. The protection of cultural heritage buildings and monuments by surface treatment with polymers is a common practice due to their ability to form a protective layer on the monument's surface as well as to control the transport of different fluids from the surface to the monument's interior. In this work, three different substrates were used: Carrara marble, Botticino limestone, and Angera stone. A commercially available Si-based resin (Alpha®SI30) was used as protective agent to improve the hydrophobicity features of the different tested materials. The surface properties of the coating and the relative interaction with the adopted stones were studied using different techniques such as contact angle measurements, electron microscope coupled with an energy dispersive spectrometer, X-ray photoelectron spectroscopy, atomic force microscopy, and attenuated total reflection infrared spectroscopy.

**Electronic supplementary material** The online version of this article (doi:10.1007/s00339-013-8127-z) contains supplementary material, which is available to authorized users.

P. Fermo (✉) · G. Cappelletti
Dipartimento di Chimica, Università degli Studi di Milano, Via Golgi 19, 20133 Milan, Italy
e-mail: paola.fermo@unimi.it

N. Cozzi
Private Laboratory, Via Dante 20, 20080 Cisliano (MI), Italy

G. Padeletti · S. Kaciulis · M. Brucale
Istituto per lo Studio dei Materiali Nanostrutturati, CNR, Monterotondo Staz, P.O. Box 10, 00015 Rome, Italy

M. Merlini
Dipartimento di Scienze della Terra, Università degli Studi di Milano, Via Botticelli 23, 20133 Milan, Italy

## 1 Introduction

The prevention of deterioration of stone materials used in works of art and in construction is of widespread interest. The deterioration process of stone monuments includes the combined action of physical, chemical, and biological factors, which induce modifications on the surface and in the structural integrity of the materials [1]. The degradation of monument places in urban area is mainly due to atmospheric pollution [2]. The best way to avoid deterioration is to prevent water penetration into the stone bulk, since accumulation of water is mainly responsible for stone decay.

Polymeric resins, acrylic polymers and copolymers, vinyl polymers, organosilicone compounds, and fluorinated materials have been applied as protective hydrophobic coatings to architectural surfaces [3–5]. More recently hybrid coatings (nano-oxides and organic composites) have been also employed [6, 7]. All these coatings allow decreasing the wettability of the surface of porous materials, reducing water penetration into stone, and therefore minimizing the rate of decay.

In the past, many hydrophobizing materials have been used and no single method has been found to be successful on all stone types. Many criteria must be met to obtain a high-performance coating, such as the reduction of water penetration, good adhesion, durability against mechanical stress and changes induced by environmental conditions, transparency, and color stability. However, the simultaneous fulfillment of these features is nowadays a challenge.

Among the hydrophobizing commercial resins, alkoxysilanes (silanes) have widely been used as protective agents. The reactions of these film-forming agents, leading to the formation of network on the surface of the monuments, have been recognized [1].

Notwithstanding numerous literature studies speak about the characteristics of the protective coatings applied, yet to our knowledge there is a poorness of specific studies concerning the specific interactions between the hydrophobic layer and the stone's surface.

Thanks to the application of techniques allowing surface analysis, in the present paper we intend to go more in detail concerning this aspect. The results concerning the physicochemical features of materials widely employed in architecture (Angera, Botticino, and Carrara stones) coated by a protective film of Alpha®SI30 (a commercial siloxane resin) will be presented and discussed. A multi-analytical approach including both bulk and surface techniques (XRD, FTIR, contact angle, SEM–EDS, XPS, and AFM) has been followed.

## 2 Experimental

Three different kinds of stone, commonly employed for monuments, were selected for the present study: Angera stone, a microcrystalline dolomite, Botticino limestone, and Carrara marble, a microcrystalline and a coarse-grained calcite, respectively. From each stone, small blocks ($1 \times 1 \times 1$ cm), coming from the quarries, were obtained and polished using carborundum paper of different sizes (220, rough surface; 1,000, smooth surface) in order to give uniform surfaces and to delete cutting imperfections.

In tables and figures the selected stones are called A (Angera), B (Botticino), and C (Carrara). The samples have been treated with a commercial water repellent protective agent, Alpha®SI30 (Sikkens) declared as an oligomeric polysiloxane by the producer on the technical note available; it is colorless, waterproof and indicated to be used on materials such as plasters and natural stones. The resin was applied as it is without any dilution. The application of the coating on the stone surfaces was carried out by using an airbrush system (Asturo airbrush, 700 μm nozzle). The quantity of sprayed coatings was kept almost constant by controlling the spray pressure (2.5 bar) and time (3 s).

The samples were characterized by laboratory X-ray powder diffraction (XRPD) technique, using a PanAlytical X'Pert instrument equipped with Cu X-ray source.

Mercury porosimetry was performed with the Porosimeter 2000 Series of ThermoFisher (0–200 Mpa) on the stones pretreated in oven overnight to remove the residual humidity.

Static contact angle (θ) measurements of water on bare and coated stones were performed on a Krüss Easy instrument. A drop of 3 μL was produced and gently placed on the surface; the drop profile was extrapolated using an appropriate fitting function. The contact angle values are well reproducible with an average standard deviation of at most 3° (the average of at least five determinations on different parts of the stones) for all the tested materials.

The samples were analyzed by electron microscopy coupled to an energy dispersive X-ray spectrometer (SEM–EDS) in order to observe the surface morphology and to study the chemical composition of the outermost layers. The instrument used was a Hitachi TM1000 equipped with an energy dispersive X-ray spectrometer (Oxford Instruments SwiftED). The spectra were acquired directly on the bare and treated stone fragments.

Infrared spectra were collected with a spectrophotometer Nicolet 380 (Thermo Electron Corporation) equipped with ATR accessory Smart Orbit (diamond crystal). IR spectra have been acquired on the resin deposited onto the ATR crystal after the evaporation of the solvent (few minutes) and after drying for 24 h, 5 and 12 days.

Both XPS and AFM measurements were performed on fragments of approximately 5 by 5 mm obtained from the marble blocks.

XPS measurements were performed in an Escalab MkII spectrometer (VG Scientific, UK) with 5 channeltron detection system and unmonochromatized Al Kα X-ray source (1486.6 eV). The electrostatic lenses were operated in large area mode, providing photoelectron collection from the sample area of about 10 mm in diameter and ensuring the maximal sensitivity of the instrument. The binding energy (BE) scale was calibrated by positioning the peak of adventitious carbon C1 s at 285.0 eV. Registered spectra were processed by Avantage v.5 software. The chemical imaging of some samples was carried out by using an Escalab 250 Xi spectrometer (Thermo Fisher Scientific, UK) equipped with monochromatized Al Kα X-ray source and combined electrostatic/magnetic lens system. After acquisition of photoemission peak (P) and background (B) images, the elemental maps were corrected for the sample topography by calculating the ratio P/(P + B) [8].

AFM imaging was performed on a Multimode 8 microscope equipped with a Nanoscope V controller and a JV piezoelectric scanner (Bruker, USA). Samples were scanned in air using Scanasyst mode with Scanasyst-Air probes (Bruker, USA). At least three different $5 \times 5$ μm areas were scanned for each sample, employing fast scan axis velocities of 2 μm $s^{-1}$ or less. Surface roughness parameters Sq (surface roughness) and Fr (surface rugosity) were obtained from the recorded images using Gwyddion 2.31.

## 3 Experimental results and discussion

The results presented in this paper are part of a larger project concerning the set-up and the study of hydrophobic coatings for the protection of stone materials. The three stones selected are commonly used in architecture and are subjected to deterioration when exposed to urban environmental pollution because of the synergic action of atmospheric pollutants and water [2].

The porosity of the stones, in terms of total open porosity, follows the sequence Angera (17 ± 1 %) > Carrara (2 ± 1 %) > Botticino (0.4 ± 0.2 %) according to the literature [9–11]. Thus, among the tested materials, Angera is the highly porous stone with a remarkable water absorption capability [12, 13].

It is well known that the application of commercial polysiloxane resins allowed obtaining hydrophobic protective coatings [7, 14, 15]. Generally, silane- and silicone-derived coatings are highly hydrophobic and in particular they maintain a high degree of permeability to water vapor [7], allowing stones to breathe and reducing deteriorations, caused by external agents, such as atmospheric pollution.

In the present case all the stones (i.e., Angera, Botticino, and Carrara), after the application of a commercial Alpha®SI30 resin, became hydrophobic: the water contact angle values increased from 50°–60° to 90°–100° (Table 1).

The XRPD analysis, performed on the neat stones, confirms the mono-mineralogical nature of the three rock samples. Angera stone is composed of dolomite, a double Ca- and Mg-carbonate [$CaMg(CO_3)_2$]. Botticino and Carrara are composed of calcite, $CaCO_3$. The dolomite and calcite minerals are clearly identified by the most intense diffraction peak at 31° (dolomite) and 29.5° (calcite). All the diffraction peaks in the pattern are indexed as dolomite or calcite (Figure S1) based on ICDD-PDF2 (International Centre for Diffraction Data, Powder Diffraction File) database (ref. 5-0586 calcite; 36-0426 dolomite). The diffraction patterns indicate for the Angera stone also a possible presence of traces of phyllosilicates (illite/mica). Carrara marble may present trace elements of dolomite and single crystal grains of pyrite, the latter identified only by optical microscopic observation.

**Table 1** Contact angle measurements on the three bare stones and on the stones coated with Alpha®SI30

| Samples | Bare stones θ (°) | Stones + Alpha®SI30 θ (°) |
|---|---|---|
| A | 53 ± 3 | 100 ± 2 |
| B | 65 ± 2 | 101 ± 2 |
| C | 64 ± 2 | 91 ± 3 |

The morphology and the elementary composition of the bare samples were investigated by SEM-EDS. SEM images (see the insets in Figure S1) show how the stone surfaces are characterized by different porosity and surface roughness, as already reported in the literature [9–11]. EDS spectra show evidence of the typical average chemical composition of the three materials (Ca and Mg for dolomite and Ca for calcite). Carrying out EDS analyses on selected points on the three surfaces, the presence of some impurities has been noticed, particularly in the case of Angera stone, which represents the most heterogeneous materials among those analyzed (see Fig. 1).

Comparing the images acquired on the bare samples with those obtained on the coated ones it can be observed how the coating is uniformly distributed on the surfaces. In particular, non-fractured films have been obtained after the resin application.

Since the producer, as concerns the chemical nature of the resin, gives a generic structure corresponding to $[R_2SiO]_n$, more information has been acquired by means of FTIR spectroscopy.

In Fig. 2a the two spectra acquired respectively on the resin dried on the ATR crystal (i.e., after solvent evaporation) and after drying for 24 h at room temperature are shown. The main peaks' assignments are reported in Table 2.

While the resin dries it begins to reticulate with the stone and this is evidenced by the shift of the band at 1,070 $cm^{-1}$ (and typical of silane, Si–O stretching) towards lower wavenumber (~1,010 $cm^{-1}$) confirming the appearance of siloxane species (Si–O–Si stretching). Thus, on the basis of IR spectra we can hypothesize that the resin is probably composed of a mixture of a trimethoxy silane (structure 1), where R could be a quite long chain (iso-octyl) (see the peak assignment in Table 2), and a PDMS (poly-dimethyl-siloxane) (structure 2).

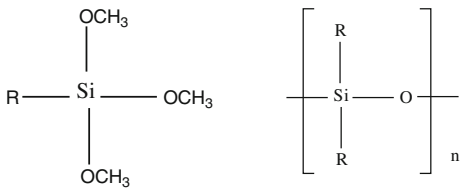


1) silane 2) PDMS

Since the signal due to siloxane could be partially overlapped to silane peak at 1,070 $cm^{-1}$, siloxane could be present also in the commercial liquid resin, as declared by the producer. It is also worth noting that after drying, the signal at 2,840 $cm^{-1}$, due to $CH_3$ stretching of the –OMe group of silane, starts to decrease (see Fig. 2b): since the

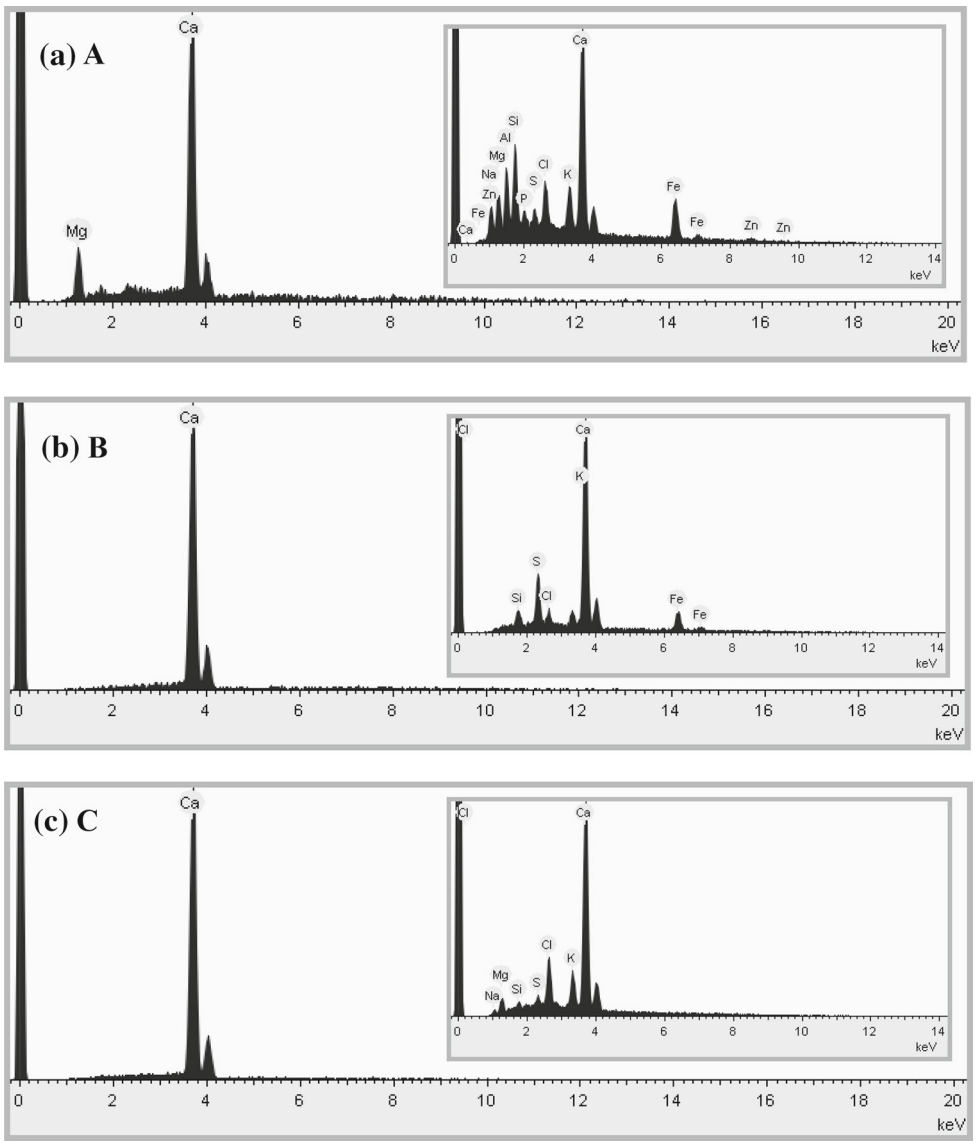


**Fig. 1** SEM-EDS spectra acquired on **a** Angera, **b** Botticino, **c** Carrara stones showing the average composition. *Insets* spectra acquired focusing the beam on single points

drying process is rather slow, a more clear decreasing of the signal is observable only after 5 days, even if after 12 days a low peak is still present. The decreasing of the intensity of the signal at 2,840 $cm^{-1}$ due to –OMe confirms that the condensation process of the resin takes place.

The formation of the links between the silane and the stone surface follows the well-known mechanism according to which the alkoxy groups of the trialkoxysilanes are hydrolyzed to form silanol-containing groups [16]. Actually, as in the most used organosilanes, Alpha®SI30 has one organic substituent and three hydrolyzable substituents. The link takes place between silane and hydroxyl groups present on the stone surfaces [16]. The nonpolar organic substitution of the silane shields the polar substrates from interaction with water. If we look at the silane effectiveness in surface modification, we can observe that it is slight towards material such as marbles [16]; nevertheless, the surface hydroxyl concentration is enough to react with the resin making the surface hydrophobic.

The usage of long chain branched R group, such as isooctyl, allows to enhance the hydrophobicity of the coating. Indeed, Wu et al. [4] attempted to modify the hydrophobicity of silane coating by incorporation of a long side C–C chain (octyl).

In order to examine the resin-stone interactions, XPS experiments were performed. No significant changes in the Ca 2p, O 1 s and C 1 s binding energies were found passing from the bare to the covered stones. Instead, specific information was obtained by comparing the Si 2p spectra of the bare and the coated stones together with the pure Alpha®SI30 resin.

Figure 3 shows the case of Angera as a representative sample: the Si 2p line for the neat stone was fit to two peaks, corresponding to silica (103.1 eV) and phyllosilicate

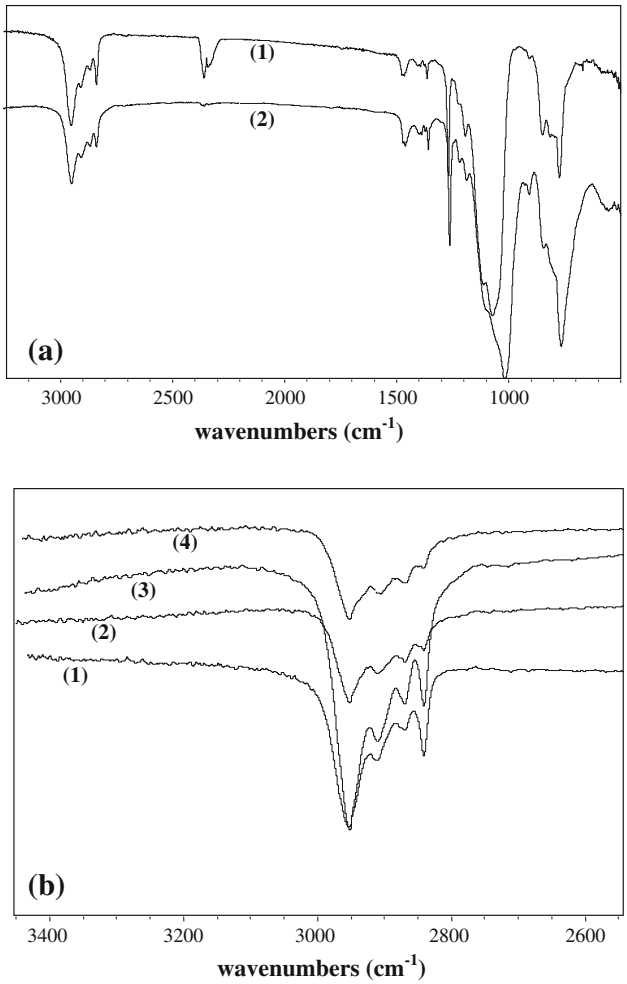


**Fig. 2** IR spectra acquired on the Alpha®SI30 resin dried on the ATR crystal (*1*), after drying for 24 h on a glass slide (*2*), after 5 days (*3*) and after 12 days (*4*). **a** Full spectra and **b** 3,400–2,500 $cm^{-1}$ region

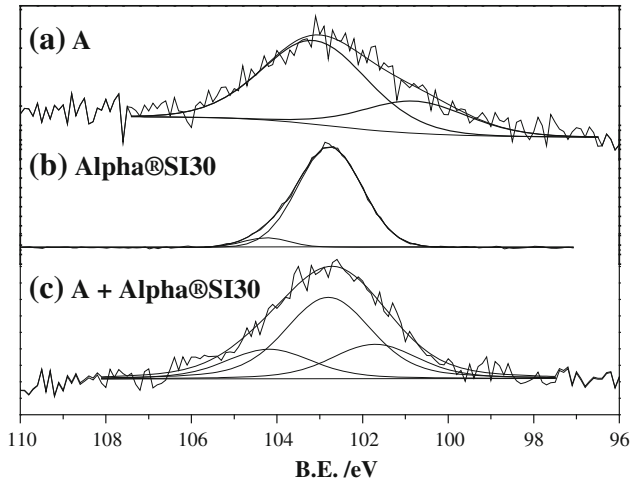


**Fig. 3** Si 2p XPS spectra of **a** the bare Angera stone, **b** the resin Alpha®SI30 deposited on a gold foil and **c** the Angera stone coated by Alpha®SI30

(100.8 eV) impurities, as reported in the literature [17–19]. This confirms the above-mentioned XRD and EDS results. No silicon species were found in the case of Botticino limestone and Carrara marble (see Table 3). The Si 2p spectrum of pure Alpha®SI30 (Fig. 3b), acquired depositing the resin on a gold foil, was deconvoluted by two peaks located at 102.8 and 104.2 eV (Table 3): the lower binding energy corresponds to the PMDS, while the higher one to the silane component of the resin [20, 21]. Actually, in the literature [22, 23], the progressive substitution of Si-R linkage (typical of $[R_2SiO]_n$) with Si–O bonds leads to a shift of the signal from 102.8 to about 104.2 eV. Figure 3c shows the Si 2p line of the Alpha®SI30-clad Angera stone: three peaks can be appreciated due to the resin (102.8 and 104.2 eV) and to the Si-based impurities (101.7 eV). The other two covered materials (Carrara and Botticino) show the same components even if slightly shifted, probably due to different resin-stone chemical surface interaction with respect to Angera stone (Table 3). The same result is reported by Douglas et al. [24] for the hydrophobization of another system (a cement paste) with silane coupling agents. They affirm that, during the condensation process,

**Table 2** Assignment of the main IR peaks observed on resin Alpha®SI30 dried on the ATR crystal

| Frequency ($cm^{-1}$) | Functional group | Comments |
|---|---|---|
| 2,950 (stretching) | $CH_3$ | Linked to Si of PDMS |
| 2,840 (stretching) | $CH_3$ | –OMe of silane; decreases when the resin is dried |
| 1,467 (bending) | $CH_2$, $CH_3$ | Aliphatic chains on silane |
| 1,396–1,377–1,364 (bending) | $CH_3$ | Split and typical of branched aliphatic chains on silane |
| 1,268 (bending) | $CH_3$ | Linked to Si of PDMS |
| 1,224 (wagging) | $CH_2$ | Linked to Si on the iso-octyl chain of silane |
| 1,193 (rocking) | $CH_3$ | –OMe of silane; decreases when the resin is dried |
| 1,072 (stretching) | Si–O | Silane, Si–O–Si of PDMS |
| 1,010 (stretching) | Si–O | Si–O–Si when the resin is dried |
| 849 (rocking) | $CH_3$ | Linked to Si of PDMS |
| 773 (stretching) | Si–C | Si–$CH_3$ on PDMS |
| 773 (rocking) | Si–$CH_2$–R | $CH_2$ on iso-octyl chain of silane |

George Socrates—Infrared and Raman Characteristic Group frequencies, 3rd Ed.—WILEY 2001

**Table 3** Assignment of Si 2p signals (BE, eV) for the different analyzed samples (bare stones A, B, C, coated stones and the pure resin)

| | Atomic ratio Si/Ca | Atomic ratio Si/Mg | Si 2p BE, eV |
|---|---|---|---|
| A | 0.17 | 1.19 | 100.8 (0.38), 103.1 (1) |
| B | – | – | – |
| C | – | – | – |
| A + Alpha®SI30 | 0.20 | 1.64 | 101.7 (0.42), 102.8 (1), 104.2 (0.36) |
| B + Alpha®SI30 | 0.66 | 7.60 | 101.6 (0.59), 102.9 (1), 104.3 (0.32) |
| C + Alpha®SI30 | 0.32 | 1.30 | 101.1 (0.31), 102.7 (1), 104.4 (0.29) |
| Alpha®SI30 | – | – | 102.8 (1), 104.2 (0.10) |

The values in brackets correspond to the relative intensities among the different Si 2p components

Si–O bonds are formed between the silane and the substrate: the B.E. of these bridging Si species is shifted with respect to the non-bridging ones, confirming the established link. In the present case, a similar behavior can be assumed.

Further, all the three treated materials show, as expected, an increase of the Si/Ca and Si/Mg atomic ratios (Table 3, 2nd and 3rd columns), suggesting that the Alpha®SI30 resin covers uniformly the stone's surface. To support these results, XPS imaging was acquired in the case of Botticino limestone (Fig. 4). After the acquisition of photoemission peak (P) and background (B) images, the images were corrected for the sample topography by calculating the ratio P/(P + B) [8]. As it can be seen from both images after topographic correction, the distribution of Ca and Si over the surface of the sample is quite uniform.

The topography of the surface stones, both pure and coated, was evaluated by AFM images. The untreated samples proved challenging due to their high roughness, which made it necessary to use extremely low scan velocities to minimize feedback artifacts. In turn, the low scan velocities implied that it was impossible to measure areas larger than a few square micrometers. All recorded images were thus 5 × 5 μm, as those found in literature for similar studies [25]. Figure 5 shows representative AFM images of sample B as it is and after different treatments, i.e., coated by brushing and dip-coating. Although mechanically polishing the surfaces might lower the overall roughness and facilitate AFM imaging, the intrinsically porosity of the samples could make this strategy largely ineffective.

All untreated samples showed a high variance of surface roughness parameters as extracted from multiple 5 × 5 μm

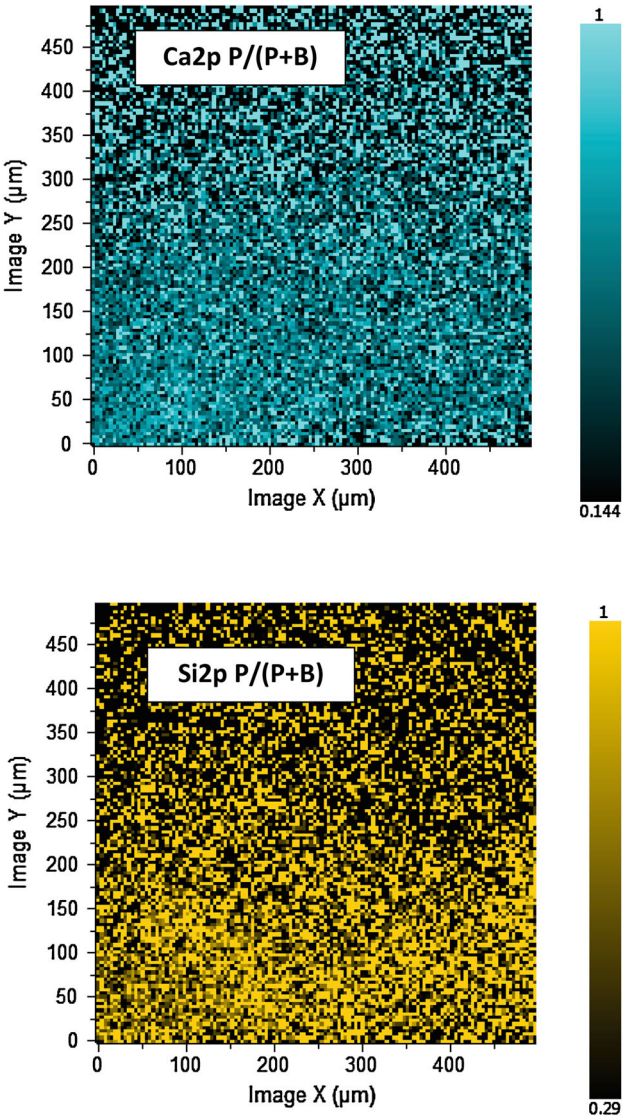


**Fig. 4** XPS imaging acquired on Botticino limestone: Ca and Si surface distributions

images recorded in different regions of the surface, in all cases revealing differences as high as a few microns between height minima and maxima within each single image. This means that the scale at which the sample's roughness can be considered homogeneous (and thus described with single scalar parameters) exceeds the maximum reliably observable area with AFM imaging. For this reason, we decided to use the standard deviation of the measurements as a rough guide to surface homogeneity (see Table 4).

No statistically significant roughness difference was detected between samples A, B, and C, nor between them and their aerograph-coated counterparts. This suggests that the sprayed coating is not thick enough to mask the material's intrinsic roughness and that the resin probably

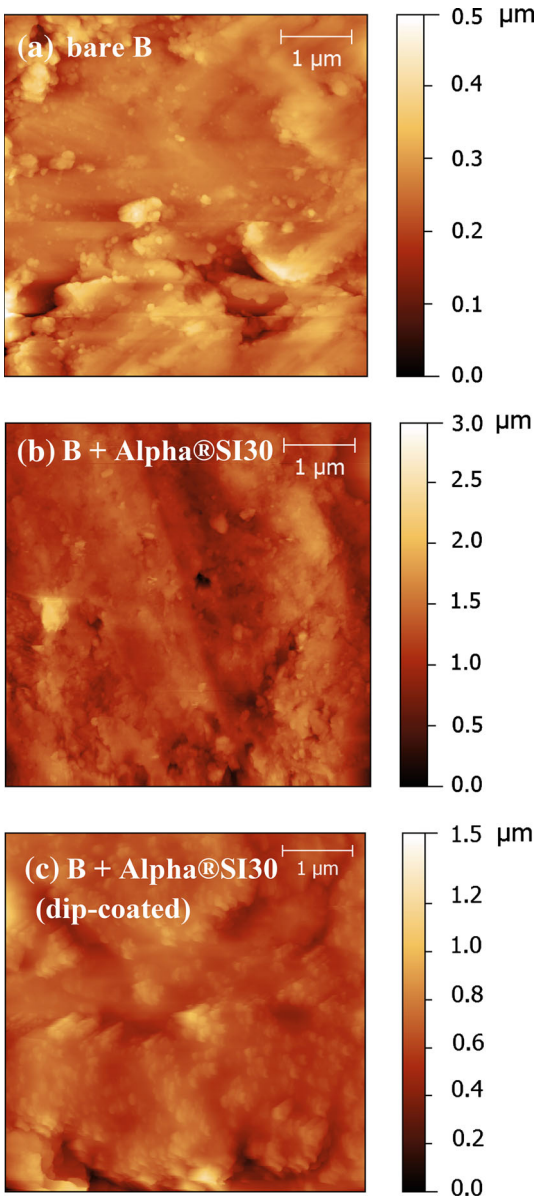


**Fig. 5** AFM images of **a** Botticino, **b** Botticino + Alpha®SI30 and **c** Botticino + Alpha®SI30 by dip-coating

**Table 4** Surface roughness parameters as determined via AFM imaging

| Sample | $S_q$ (nm) | $F_r$ |
|---|---|---|
| B | 162 ± 119 | 3 ± 2 |
| B + Alpha®SI30 | 201 ± 94 | 2 ± 1 |
| B + Alpha®SI30 (dip-coated) | 99 ± 2 | 1.13 ± 0.04 |

The standard deviation from multiple measurements performed on the same sample is used as the error (see main text). Surface roughness $S_q$ is defined as the average root mean square deviation from the arithmetic average of Z values in each measured 5 × 5 μm area. Surface rugosity $F_r$ is defined as the ratio between the apparent surface area and the area projected on the *xy* plane (25 $\mu m^2$ for all recorded images)

forms a thin film following the features of the samples. Conversely, dip-coated samples showed an extremely (two orders of magnitude) lower variance in roughness parameters, validating the use of scalar roughness parameters (see Table 4). This suggests that in this case, the resin is flooded into the surface, effectively masking the texture of the stones and offering a smooth surface for the analysis.

## 4 Conclusions

Surface coatings obtained applying a commercial siloxane resin, Alpha®SI30, to stones normally used in architecture (i.e., Angera, Botticino, and Carrara) have been characterized following a multi-analytical approach based on the use of both bulk and surface techniques. The coatings obtained turned out to be hydrophobic, as demonstrated by contact angle measurements. Furthermore, SEM observations have shown that the surfaces were homogeneous from a microscopic point of view and without cracks or fractures. The resin composition has been disclosed by ATR spectroscopy and it resulted in a mixture of a trimethoxy silane, where R could be a quite long chain (iso-octyl), and PDMS (poly-dimethyl-siloxane). The reticulation process has been also highlighted. From XPS analyses, the different types of Si are evident, thus confirming the observations by ATR. XPS also showed evidence of the quite homogeneous distribution of the resin over the stones. The topography of the surfaces has been investigated by AFM and it has been observed that the sprayed coating was not thick enough to mask the material roughness and that the resin probably forms a thin film following the features of the samples.

## References

1. C.A. Price, *Stone conservation* (The Getty Conservation Institute, Los Angeles, 1996)
2. P. Brimblecombe, in *Urban air pollution European aspects*, ed. by J. Finger, O. Herter, F. Palmer (Kluver, Dordrecht, 1999), pp. 7–20
3. L. Toniolo, T. Poli, V. Castelvetro, A. Manariti, O. Chiantore, M. Lazzari, J Cult Herit **3**, 309 (2002)
4. L.Y.L. Wu, A.M. Soutar, X.T. Zeng, Surf Coat Technol **198**, 420 (2005)
5. O. Chiaronte, M. Lazzari, Polymer **42**, 17 (2001)
6. M.F. La Russa, S.A. Ruffolo, N. Rovella, C.M. Belfiore, A.M. Palermo, M.T. Guzzi, G.M. Crisci, Progr. Org. Coat. **74**, 186 (2012)
7. C. Kapridaki, P. Maravelaki-Kalaitzaki, Progr. Org. Coat. **76**, 400 (2013)
8. A. Carosi, M. Amati, L. Gregorati, S. Kaciulis, A. Mezzi, R. Montanari, L. Rovatti, N. Ucciardello, Surf Interface Anal **42**, 726 (2010)
9. M. Gombia, V. Bortolotti, R.J.S. Brown, M. Camaiti, L. Cavallero, P. Fantazzini, J. Phys. Chem. B **113**, 10580 (2009)

10. E. Cantisani, E. Pecchioni, F. Fratini, C.A. Garzonio, P. Malesani, G. Molli, Int. J. Rock. Mech. Min. Sci. **46**, 128 (2009)
11. T. Poli, L. Toniolo, O. Chiantore, Appl. Phys. A **79**, 347 (2004)
12. G. Alessandrini, R. Bugini, R. Peruzzi, *I materiali lapidei impiegati nei monumenti lombardi ed i loro problemi di conservazione. Materiali lapidei: problemi relativi allo studio del degrado e della conservazione* (Istituto Poligrafico dello Stato, Rome, 1987)
13. D. Gulotta, M. Bertoldi, S. Bortolotto, P. Fermo, A. Piazzalunga, L. Toniolo, Env. Earth Sci. **69**, 1085 (2013)
14. G. Soliveri, R. Annunziata, S. Ardizzone, G. Cappelletti, D. Meroni, J. Phys. Chem. C **116**, 26405 (2012)
15. F. Milanesi, G. Cappelletti, R. Annunziata, C.L. Bianchi, D. Meroni, S. Ardizzone, J. Phys. Chem. C **114**, 8287 (2010)
16. B. Arkles, Chem. Tech. **7**, 766 (1977)
17. J.F. Moulder, W.F. Stickle, K.D. Bomben, *Handbook of X-ray photoelectron spectroscopy* (Perkin-Elmer, Eden Praire, 1992)
18. C.D. Wagner, H.A. Six, J.A. Taylor, W.T. Jansen, Appl. Surf. Sci. **9**, 203 (1981)
19. A. Oya, F. Beguin, K. Fujita, R. Benoit, J. Mater. Sci. **31**, 4609 (1996)
20. V. Sunkara, Y.-K. Cho, Appl. Mater. Interfaces **4**, 6537 (2012)
21. Y. Zhu, M. Otsubo, C. Honda, S. Tanaka, Polym. Degrad. Stabil. **91**, 1448 (2006)
22. M.R. Alexander, R.D. Short, F.R. Jones, W. Michaeli, C.J. Blomfield, Appl. Surf. Sci. **137**, 179 (1999)
23. L.-A. O'Hare, A. Hynes, M.R. Alexander, Surf. Interface Anal. **39**, 926 (2007)
24. A. Stewart, B. Schlosser, E.P. Douglas, Appl. Mater. Interfaces **5**, 1218 (2013)
25. P.N. Manoudis, A. Tsakalof, I. Karapanagiotis, I. Zuburtikudis, C. Panayiotou, Surf. Coat Technol. **203**, 1322 (2009)



View publication stats